

Article

Analysis of Genomic Alternative Splicing Patterns in Rat under Heat Stress Based on RNA-Seq Data

Shangzhen Huang ¹, Jinhuan Dou ^{2,*}, Zhongshu Li ³, Lirong Hu ¹, Ying Yu ¹ and Yachun Wang ^{1,*}

¹ National Engineering Laboratory of Animal Breeding, Key Laboratory of Animal Genetics, Breeding and Reproduction, MARA, College of Animal Science and Technology, China Agricultural University, Beijing 100193, China; hsz19980225@163.com (S.H.); b20193040324@cau.edu.cn (L.H.); yuying@cau.edu.cn (Y.Y.)

² Animal Science and Technology College, Beijing University of Agriculture, Beijing 100193, China

³ Agricultural College, Yanbian University, Yanji 133002, China; lizhongshu@ybu.edu.cn

* Correspondence: doujinhuan@bua.edu.cn (J.D.); wangyachun@cau.edu.cn (Y.W.)

Abstract: Heat stress is one of the most severe challenges faced in livestock production in summer. Alternative splicing as an important post-transcriptional regulation is rarely studied in heat-stressed animals. Here, we performed and analyzed RNA-sequencing assays on the liver of Sprague-Dawley rats in control (22 °C, $n = 5$) and heat stress (4 °C for 120 min, H120; $n = 5$) groups, resulting in the identification of 636 differentially expressed genes. Identification analysis of the alternative splicing events revealed that heat stress-induced alternative splicing events increased by 20.18%. Compared with other types of alternative splicing events, the alternative start increased the most (43.40%) after heat stress. Twenty-eight genes were differentially alternatively spliced (DAS) between the control and H120 groups, among which *Acly*, *Hnrnpd* and *mir3064* were also differentially expressed. For DAS genes, *Srebfl1*, *Shc1*, *Srsf5* and *Ensa* were associated with insulin, while *Cast*, *Srebfl1*, *Tmem33*, *Tor1aip2*, *Slc39a7* and *Sqstm1* were enriched in the composition of the endoplasmic reticulum. In summary, our study conducts a comprehensive profile of alternative splicing in heat-stressed rats, indicating that alternative splicing is one of the molecular mechanisms of heat stress response in mammals and providing reference data for research on heat tolerance in mammalian livestock.

Keywords: heat stress response; post-transcriptome; alternative splicing; liver; rat



Citation: Huang, S.; Dou, J.; Li, Z.; Hu, L.; Yu, Y.; Wang, Y. Analysis of Genomic Alternative Splicing Patterns in Rat under Heat Stress Based on RNA-Seq Data. *Genes* **2022**, *13*, 358. <https://doi.org/10.3390/genes13020358>

Academic Editor: Paolo Cinelli

Received: 17 December 2021

Accepted: 15 February 2022

Published: 16 February 2022

Publisher's Note: MDPI stays neutral with regard to jurisdictional claims in published maps and institutional affiliations.



Copyright: © 2022 by the authors. Licensee MDPI, Basel, Switzerland. This article is an open access article distributed under the terms and conditions of the Creative Commons Attribution (CC BY) license (<https://creativecommons.org/licenses/by/4.0/>).

1. Introduction

The non-specific response of an organism caused by excessively high environmental temperature is called heat stress [1] and it usually occurs when the ambient temperature is above the upper critical temperature of the thermal neutral zone. The efficiency of livestock products is compromised under heat stress conditions, since nutrients are diverted to maintain eutheria [2]. The cumulative impacts of heat stress on feed intake, metabolism and physiology status may result in reduced milk yield in dairy cattle [3], decreased body weight and growth rate in broiler [4], pig [5], lamb [6] and beef cattle [3]. Furthermore, heat stress has detrimental effects on both male and female reproductive functions [7] and threatens animal health and welfare [8]. According to a survey, heat stress has placed a huge economic burden on the animal husbandry industry [9], e.g., in the United States alone, the loss of dairy induced by heat stress is approximately \$900 million/year and the loss of beef and swine exceeds \$300 million/year.

To the best of our knowledge, the temperature–humidity index (THI) is usually used as the environmental index in heat stress studies [10]. Different species have different THI thresholds for determining the occurrence of heat stress [11]. The THI reflects the heat stress of a population from an environmental perspective, but at an individual level, few accurate markers have been used in the prediction of heat stress, which may be largely related to the fact that the molecular mechanism regulating heat stress is not clear. With the

development of next-generation sequencing technology, numerous studies (including our previous studies) have identified lots of heat stress-related genes using RNA-sequencing (RNA-Seq) [12–17], but transcriptome information is still incomplete. A comprehensive analysis of alternative splicing of transcripts is lacking. The phenomenon of alternative splicing of genes was first proposed in 1978, that is, a pre-mRNA generates multiple different mRNA isoforms by selecting different splicing sites [18]. Alternative splicing is a ubiquitous mechanism in higher eukaryotes and contributes to both transcriptome and proteome diversity [19,20]. In addition, alternative splicing is involved in many physiological processes, as well as responses to biotic and abiotic stresses [21–25].

Studies on alternative splicing of heat-stressed animals have been carried out. As early as 1994, Takechi et al. detected that heat stress caused alternative 5' splice site selection of *HSP47* in mice [26]. The activation of potential alternative 5' splice sites induced by heat stress is widespread in the human genome [27] and regulated by the suppression of splicing mechanisms [28]. The ratio of alternative splicing isoforms of *TLR4* in Bama minipig (*Sus scrofa domestica*) [29] and *dHSF* in *Drosophila* [30] are changed after heat stress. Kaitsuka et al. found that eEF1B δ changes its structure and function from a translation factor into a heat-shock response transcription factor by alternative splicing and induces heat-shock element (HSE)-containing genes [31]. In addition, Tan et al. conducted the first comprehensive study on alternative splicing in heat-stressed fish in 2019 [32]. As far as we know, there has not been a comprehensive transcriptome study to identify heat stress-induced alternative splicing changes in mammals.

Based on the heat-stressed rat model that was built in our previous study [14], a comprehensive analysis of alternative splicing rules was performed in the current study. After the bioinformatic analysis, the differentially expressed genes (DEGs) and differentially alternatively spliced (DAS) genes were identified and important biological processes involved in the heat stress response were analyzed. This work further provides reference data for research on heat tolerance in mammalian livestock.

2. Materials and Methods

2.1. Animals and Treatments

The in vivo rat experiments were performed at the College of Animal Science and Technology, China Agricultural University. The Institutional Animal Care and Use Committee approved all the experimental procedures, which complied with the China Physiological Society's guiding principles for research involving animals and adhered to the high standard (best practice) of veterinary care as stipulated in the Guide for Care and Use of Laboratory Animals.

In previous research [14], 99 eight-week old female specific-pathogen-free (SPF) Sprague-Dawley rats (Beijing Vital River Laboratory Animal Technology Co., Ltd., Beijing, China) weighing 205 ± 7.16 g were used as subjects. Prior to the experiments, a total of three rats per cage were housed in Nalgene polycarbonate cages ($40 \times 30 \times 180$ cm³, Beijing Vital River Laboratory, Animal Technology Co, Ltd., Beijing, China) at 22 ± 1 °C and 50% relative humidity (RH) with a 12 h reverse light/dark cycle (on 06:00, off 18:00) for one week. Rats were given access to feed and water ad libitum and all experiments were conducted with healthy and conscious rats. As previously described [14], five rats randomly assigned to the heat stress group were exposed to 42 °C for 120 min (H120) and five rats in the control group were reared at 22 ± 1 °C. The heating experiments were completed in a floor-standing artificial climate incubator (BIO250, BOXUN Medicine Instrument Co, Shanghai, China). Rats in the control group were never introduced into the incubator. After treatments, the rats were anesthetized by intraperitoneal injection of 1%, 1.2 mL sodium pentobarbital (40 mg/kg of body weight) and liver tissues were collected. Liver tissues were washed in ice-cold phosphate buffer solution (PBS) and snap-frozen immediately in liquid nitrogen until further analysis.

2.2. RNA Extraction, cDNA Library Construction and Illumina Deep Sequencing

Total RNA was extracted from quick-frozen liver samples using TRIzol[®] reagent (Invitrogen Life Technologies, Palo Alto, CA, USA), according to the manufacturer instructions. After homogenising the sample with TRIzol[®] Reagent, chloroform was added, RNA was precipitated with isopropanol, then treated with 75% ethanol [33,34]. The total RNA was dissolved using DNase/RNase-free water. The RNA quality and quantity were determined using agarose gel electrophoresis and NanoDrop 2000 (Thermo Fisher Scientific, Waltham, MA, USA). The RNA integrity was assessed using the RNA Nano 6000 Assay Kit in the Agilent Bioanalyzer 2100 system (Agilent Technologies, Santa Clara, CA, USA). Then, the mRNA was purified and enriched from total RNA using Poly-T oligo-attached magnetic beads and sheared into fragments. First-strand cDNA was generated using random hexamer primers and M-MuLV Reverse Transcriptase (RNase H). Second-strand cDNA was synthesized using DNA polymerase I and RNase H. The library fragments were purified with the AMPure XP system (Beckman Coulter, Beverly, MA, USA) to select cDNA fragments approximately 200 bp in length and PCR amplified. Finally, the library was sequenced in paired-end 150 bp reads using the Illumina[®] HiSeq 2000 platform.

2.3. Data Filtering and Transcriptome Alignment

The raw reads were filtered by removing the adapter sequences; reads with poly-N and low-quality reads (i.e., more than 50% of the reads with a quality score under 10 or read length <30) were trimmed using Trim Galore 0.4.5 (http://www.bioinformatics.babraham.ac.uk/projects/trim_galore/ (accessed on 12 February 2020)) and FastQC 0.11.8 [35] software. In addition, Q20, Q30 and GC content were calculated to evaluate data quality. High-quality reads were aligned to the rat reference genome (*Rattus norvegicus* 6.0.98, Rnor 6.0.98) using STAR 2.5.3 [36] with the default parameters. Only reads uniquely aligned to the reference genome were used for downstream analysis.

2.4. Identification of Differential Expression Genes

The aligned reads were assembled using the StringTie 1.3.5 [37]. The *stattest* function in Ballgown 3.11 [38] was applied to identify DEGs between the Control and H120 groups. The expression levels of the genes were normalized with FPKM (fragments per kilobase per million mapped fragments). Genes with BH-adjusted *p*-value (*q*-value) < 0.05 and $|\log_2\text{FoldChange}| > 1$ were considered as DEGs.

2.5. Identification of Differential Alternative Splicing Events

Alternative splicing patterns were analyzed using SGSeq 1.22.0 [39] via estimating the percent spliced in (PSI) for each variant, taking “TxDb.Rnorvegicus.UCSC.rn6.refGene” as the reference genome. A PSI greater than 0 and less than 1 indicates that this alternative splicing event occurred on the sample level. The *t*-test was used to compare the difference in the number of events between the Control and H120 groups. For each group, the alternative splicing events that occurred in at least three samples were retained at the group level. Eight types of alternative splicing events were distinguished, including alternative 5' splice site (A5SS), alternative 3' splice site (A3SS), skipped exon (SE), retained intron (RI), mutually exclusive exons (MXE), alternative start (AS), alternative end (AE) and unknown type.

The DEXSeq 3.11 [40] was used to perform a statistical test for differential variant usage between the Control and H120 groups. A BH-adjusted *p*-value (*q*-value) < 0.05 and differences in PSI values (dPSI) between conditions > 0.1 were set as criteria to filter DAS events. Genes with at least one DAS event were determined as DAS genes.

2.6. Integrated Gene Expression and Alternative Splicing Results

The clustering analysis of DEGs and DAS genes was performed using Venn2.1 (<https://bioinfogp.cnb.csic.es/tools/venny/> (accessed on 28 August 2021)). The overlapped genes were considered as DAS genes with different expression levels between the Control and H120 groups. A hypergeometric distribution test was performed in order to test

whether the overlap was significant (<https://systems.crumpl.ucla.edu/hypergeometric/> (accessed on 28 August 2021)). In order to obtain protein structure information (tertiary structure score) and functional information (number of functional residues and domain score) of the overlapping genes, the APPRIS Database [41] was employed to annotate the alternative splicing isoforms of these genes.

2.7. Functional Analysis of Differentially Expressed Genes and Differentially Alternatively Spliced Genes

The functional enrichment analysis of DEGs and DAS genes considering Gene Ontology (GO) terms and the Kyoto Encyclopedia of Genes and Genomes (KEGG) pathway was conducted using DAVID v.6.8 [42]. Results with a false discovery rate (FDR) value < 0.05 for DEGs and a *p*-value < 0.05 for DAS genes were considered as significant. The functions of DAS genes with significant different expression levels were further searched in the UniProt Knowledgebase [43] and the Rat Genome Database [44].

2.8. Validation of the Expression Level of the DAS Genes by Real-Time Quantitative PCR

The RNA of the liver was transcribed into cDNA using the PrimeScript RT reagent Kit with gDNA Eraser (Takara). The primers of five randomly selected DAS genes are listed in Supplementary Table S1, and the glyceraldehyde-3-phosphate dehydrogenase gene (*GAPDH*) was used as the internal reference gene. Primers for *GAPDH* and DAS genes were designed using Primer-BLAST (<https://www.ncbi.nlm.nih.gov/tools/primer-blast/> (accessed on 30 December 2020)) [45], and primers were synthesized by Beijing Tsingke Biological Technology (Beijing, China). Each reaction was performed in 20 mL mixtures, including a 2 mL diluted cDNA sample as template, 10 mL SYBR Green I Master (Roche), 0.6 mL forward and 0.6 mL reverse gene-specific primers, and 6.8 mL ddH₂O. Amplification conditions were set as follows: denaturation at 95 °C for 10 min, followed by 40 cycles of 98 °C for 10 s and 60 °C for 20 s for annealing, and extension at 72 °C for 20 s, followed by a final extension at 65 °C for 1 min. Triplicate real-time quantitative PCRs (RT-qPCR) were accomplished for each cDNA sample. The comparative threshold cycle (Ct) value method was adopted to analyze relative gene expression. The Pearson correlation coefficients between the FPKM counts from the RNA-Seq analysis and expression levels relative to *GAPDH* from the RT-qPCR analysis were calculated.

3. Results

3.1. Summary of the Basic Information

The average of the total paired-end raw reads of the samples was 31,106,148 bp (ranging from 26,255,321 to 38,816,107 bp), and the average of high-quality clean data after data filtering was 30,565,891 bp with a GC content of 49.73% (Supplementary Table S2). The average percentages of Q20 and Q30 were 94.95% and 89.34%, respectively. After alignment analysis, the total mapped rates ranged from 94.69% to 97.88% among all samples. Bioinformatic analysis for high-throughput transcriptome data revealed a total of 10,707 genes annotated in the liver tissues.

3.2. Identification of Differentially Expressed Genes

A total of 636 DEGs were identified in the comparison of Control vs. H120, among which 374 genes were upregulated and 262 genes were downregulated (Figure 1 and Supplementary Table S3). The top five DEGs includes two upregulated genes (*Mical2* and *Arl5b*) and three downregulated genes (*Paqr7*, *Rmnd5b* and *Alpl*). There were seven DEGs with $|\log_2\text{FoldChange}| > 3.5$, among which the expression levels of *Hspa1b* and *Hspb1* in the H120 group were 152.63 and 11.53 times higher than those in the Control group, respectively.

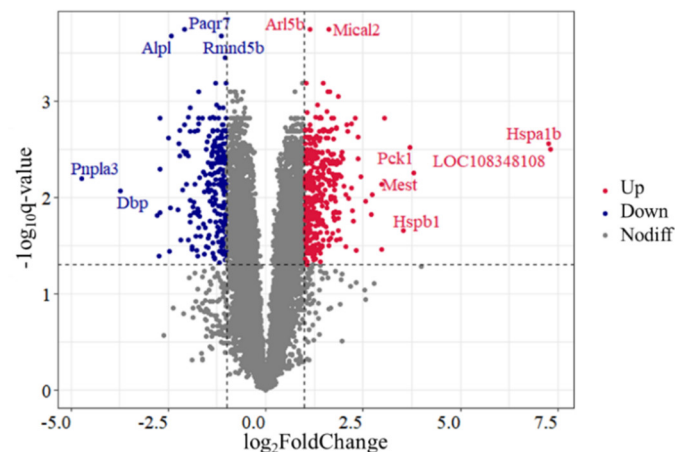


Figure 1. Volcano plot of differentially expressed genes (DEGs) identified in rat liver tissues in the Control and H120 groups. Up and Down represent that the expression levels of DEGs were significantly (q -value < 0.05 and $|\log_2\text{FoldChange}| > 1$) higher and lower in the H120 group compared with the Control, respectively. Nodiff means the expression levels of genes are not significantly different between the Control and H120 groups. The DEGs with a q -value < 0.0003 or $|\log_2\text{FoldChange}| > 3.5$ were marked with gene names.

3.3. Functional Enrichment Analysis for Differentially Expressed Genes

Functional enrichment analysis of DEGs revealed that a total of eleven biological processes (BP), six cellular components (CC) and one molecular function (MF) were significantly enriched (FDR value < 0.05) (Figure 2 and Supplementary Table S4). Genes such as *Dnaja1*, *Socs3*, *Hspa8*, *Hsp90aa1*, *Eif2b3*, *Abcc2*, *Pklr*, *Dnaja4*, *Tp53inp1*, *Loc103692716* and *Hspa1b* were found to be related to the biological process of response to heat (GO:0009408). Furthermore, thirty-nine genes had the function of regulating the oxidation–reduction process (GO:0055114). In total, ten KEGG pathways were significantly enriched (FDR value < 0.05) (Figure 2 and Supplementary Table S4), including biosynthesis of antibiotics (rno01130) as the most significant pathway. A total of 62 DEGs were involved in metabolic pathways (rno01100), especially in pyruvate metabolism (rno00620), carbon metabolism (rno01200) and fatty acid metabolism (rno01212).

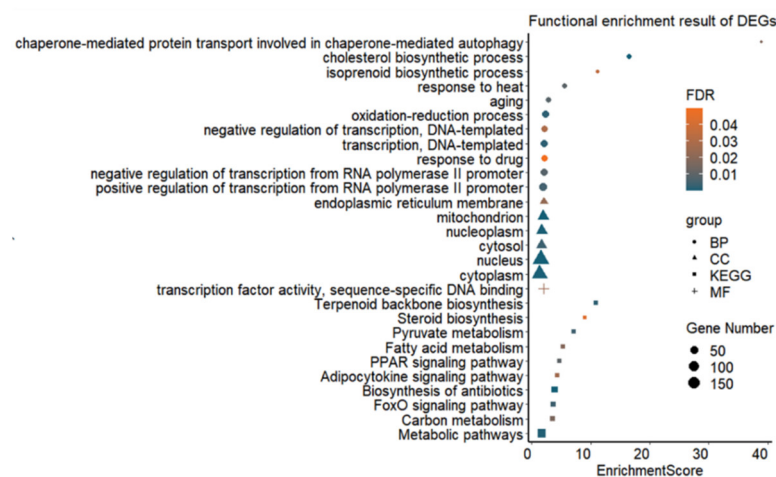


Figure 2. Significantly enriched GO terms and pathways for DEGs in rat liver tissues in the Control (22 °C, $n = 5$) and heat stress (42 °C for 120 min, H120; $n = 5$) groups. BP = biological process, CC = cellular component, MF = molecular function, KEGG = Kyoto Encyclopedia of Genes and Genomes pathway, FDR = false discovery rate.

3.4. Summary of Alternative Splicing Events

The number of alternative splicing events that occurred in each sample is shown in Figure 3. At the sample level, an average of 273 and 311 alternative splicing events were identified from the Control and H120 groups, respectively. The difference between the Control and H120 groups was not significant ($p = 0.1$). At the group level, a total of 228 alternative splicing events occurred in the liver of the Control, corresponding to 220 genes; 274 alternative splicing events occurred in the liver of the H120, corresponding to 256 genes, showing that heat stress-induced alternative splicing events increased by 20.18%, the corresponding alternatively spliced genes increasing by 16.36%.

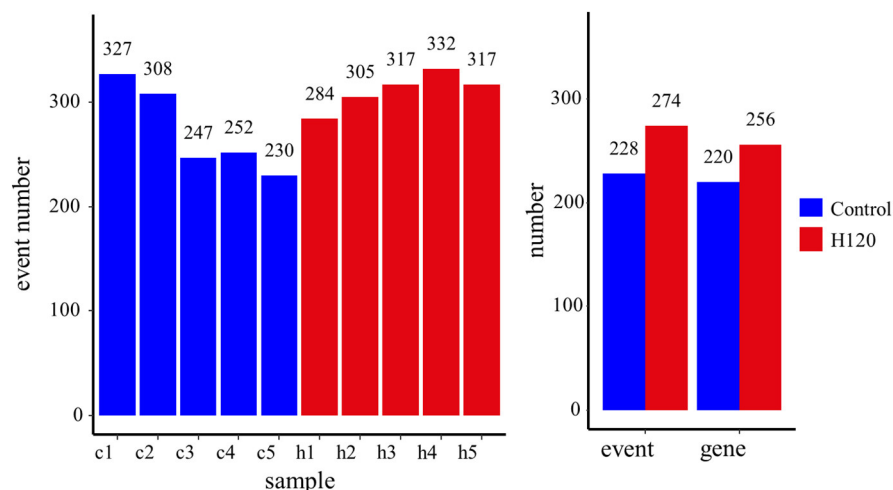


Figure 3. The alternative splicing events identified at the sample level and the group level. Samples c1–c5 are liver tissue samples of rats in the Control group and samples h1–h5 are from the H120 group.

Eight types of alternative splicing events were identified in the Control and H120 groups (Table 1). In detail, AS accounts for the highest proportion of the two groups (23% in Control and 27% in H120), followed by SE (20% in Control and 21% in H120). The proportion of other types of events is between 10% and 15%, except for MXE and an unknown event at less than 5%. The number of all types of alternative splicing events increased after heat stress except for RI. AS increased the most after heat stress, from 53 to 76.

Table 1. The number of all types of alternative splicing events in Control and H120 groups.

	A3SS	A5SS	MXE	RI	SE	AS	AE	Unknown
Control	28	32	8	32	47	53	26	6
H120	31	35	11	31	57	76	28	8
Increase (%)	10.71	9.38	37.50	−3.12	21.28	43.40	7.69	33.33

A3SS = alternative 3' splice site, A5SS = alternative 5' splice site, MXE = mutually exclusive exons, RI = retained intron, SE = skipped exon, AS = alternative start, AE = alternative end. Increase (%) = (the number of events in H120 group—the number of events in Control group)/the number of events in Control group.

3.5. Identification of Differential Alternative Splicing Events and Genes

Forty alternative splicing events had a q -value < 0.05 , including 26 events with $dPSI > 0.1$, which were considered to be DAS events (Table 2), with six AS, five AE, four SE, four RI, three A5SS, two A3SS, as well as one each for MXE and unknown. A single variant of some DAS genes (*Cast*, *Hnrnpf*, *Srsf5*, *Hnrnpd*, *Crem* and *Zmynd11*) corresponds to multiple transcripts, indicating that there was at least one alternative splicing event in other positions of the gene. The *Ngrn*'s alternative splicing event produces non-coding transcripts. It can be seen from the Figure 4a that the samples of each group were clustered together according to PSI, and there were significant differences between the Control and H120 groups. The $dPSI$ values of *Abcg3l2*, *Abcg3l4*, *Tor1aip2*, *Cast* and *Zmynd11* were all

greater than 0.35. The $|\log_2\text{FoldChange}|$ of five DAS genes in the H120 and Control groups generated by RT-qPCR were in line with the results of the RNA-Seq data (Figure 4b). The Pearson correlation coefficient between RT-qPCR and RNA-Seq was as high as 0.95, which confirmed the reliability of the RNA-Seq analysis.

Table 2. Summary of information for the differential alternative splicing events.

Gene Symbol	Start	End	Type	Transcription	q-Value	dPSI
<i>Strn4</i>	chr1:78756007:+	chr1:78756355:+	A3SS:P	NM_001107480	0.0481	0.20
<i>Strn4</i>	chr1:78756007:+	chr1:78756355:+	A3SS:D	NM_001161809	0.0494	−0.20
<i>Ngrn</i>	chr1:142050672:+	chr1:142051084:+	RI:E	NM_001033900	0.0031	−0.16
<i>Ngrn</i>	chr1:142050672:+	chr1:142051084:+	RI:R	NR_028055	0.0031	0.16
<i>Wbp11</i>	chr1:266401987:+	chr1:266409945:+	A5SS:D	NM_001127484	0.0024	−0.10
<i>Wbp11</i>	chr1:266401987:+	chr1:266409945:+	A5SS:P	NM_001313908	0.0024	0.10
<i>Shc1</i>	chr2:188745503:+	chr2:188748894:+	AS	NM_053517	0.0048	−0.17
<i>Shc1</i>	chr2:188748359:+	chr2:188748894:+	AS	NM_001164060	0.0048	0.17
<i>Ensa</i>	chr2:197756356:+	chr2:197759882:+	AE	NM_021842	0.0000	−0.24
<i>Ensa</i>	chr2:197756356:+	chr2:197758162:+	AE	NM_001033974	0.0000	0.24
<i>Cast</i>	chr2:1506234:−	chr2:1501715:−	SE:S	NM_001033716	0.0000	0.39
<i>Cast</i>	chr2:1506234:−	chr2:1501715:−	SE:I	NM_001033715 NM_053295	0.0000	−0.39
<i>Hnrnpf</i>	chr4:149957206:+	chr4:149970689:+	AS	NM_001037287	0.0051	−0.31
<i>Hnrnpf</i>	chr4:149970237:+	chr4:149970689:+	AS	NM_001037285 NM_022397	0.6048	0.08
<i>Hnrnpf</i>	chr4:149970567:+	chr4:149970689:+	AS	NM_001037286	0.0168	0.23
<i>Ak2</i>	chr5:147200851:+	chr5:147204050:+	AE	NM_001033967	0.0165	−0.10
<i>Ak2</i>	chr5:147200851:+	chr5:147201014:+	AE	NM_030986	0.0165	0.10
<i>Ppm1b</i>	chr6:8261060:+	chr6:8271055:+	AE	NM_001270619	0.0165	0.14
<i>Ppm1b</i>	chr6:8261060:+	chr6:8273549:+	AE	NM_033096	0.8322	0.04
<i>Ppm1b</i>	chr6:8261060:+	chr6:8280124:+	AE	NM_001270620	0.0000	−0.17
<i>Srsf5</i>	chr6:104611145:+	chr6:104612019:+	A5SS:D	NM_001195506	0.0000	−0.21
<i>Srsf5</i>	chr6:104611145:+	chr6:104612019:+	A5SS:P	NM_019257 NM_001195505	0.0000	0.21
<i>Tcf3</i>	chr7:12164343:+	chr7:12167727:+	Unknown	NM_001035237	0.0013	0.15
<i>Tcf3</i>	chr7:12164343:+	chr7:12167727:+	Unknown	NM_133524	0.0013	−0.15
<i>Nabp2</i>	chr7:2825608:−	chr7:2825124:−	AS	NM_001244819	0.0261	−0.18
<i>Nabp2</i>	chr7:2825498:−	chr7:2825124:−	AS	NM_001034939	0.0261	0.18
<i>Sqstm1</i>	chr10:35713296:−	chr10:35704728:−	AE	NM_175843	0.0000	−0.24
<i>Sqstm1</i>	chr10:35713296:−	chr10:35713103:−	AE	NM_181550	0.0000	0.24
<i>Srebfl</i>	chr10:46582854:−	chr10:46579444:−	AS	NM_001276708	0.0168	−0.14
<i>Srebfl</i>	chr10:46593009:−	chr10:46579444:−	AS	NM_001276707	0.0172	0.14
<i>Acly</i>	chr10:88419161:−	chr10:88413611:−	SE:S	NM_001111095	0.0000	0.33
<i>Acly</i>	chr10:88419161:−	chr10:88413611:−	SE:I	NM_016987	0.0000	−0.33
<i>Ddx5</i>	chr10:94988461:−	chr10:94982051:−	AS	NM_001007613	0.0000	−0.34
<i>Mir3064</i>	chr10:94982117:−	chr10:94982051:−	AS	NR_128673	0.0000	0.34
<i>Zcchc2</i>	chr13:26000532:+	chr13:26014926:+	AE	NM_001122677	0.0013	−0.29
<i>Zcchc2</i>	chr13:26000532:+	chr13:26000769:+	AE	NM_001271042	0.0015	0.29
<i>Tor1aip2</i>	chr13:73708912:+	chr13:73718239:+	SE:S	NM_001165897	0.0000	0.39
<i>Tor1aip2</i>	chr13:73708912:+	chr13:73718239:+	SE:I	NM_001165896	0.0000	−0.39
<i>Ephx1</i>	chr13:99287887:−	chr13:99284094:−	AS	NM_012844	0.0000	0.18
<i>Ephx1</i>	chr13:99300580:−	chr13:99284094:−	AS	NM_001034090	0.0000	−0.18
<i>Hnrnpd</i>	chr14:11256779:+	chr14:11268562:+	SE:S	NM_001082539 NM_001082541	0.0403	0.23
<i>Hnrnpd</i>	chr14:11256779:+	chr14:11268562:+	SE:I	NM_001082540 NM_024404	0.0403	−0.23
<i>Abcg314</i>	chr14:5794507:−	chr14:5607839:−	MXE	NM_001037205	0.0022	0.51
<i>Abcg312</i>	chr14:5794507:−	chr14:5607839:−	MXE	NM_001014133	0.0022	−0.51
<i>Tmem33</i>	chr14:42540006:−	chr14:42539079:−	RI:E	NM_001034198	0.0037	−0.14

Table 2. Cont.

Gene Symbol	Start	End	Type	Transcription	q-Value	dPSI
<i>Tmem33</i>	chr14:42540006:–	chr14:42539079:–	RI:R	NM_021671 NM_001110860	0.0037	0.14
<i>Crem</i>	chr17:57082726:+	chr17:57088162:+	A3SS:P	NM_001271247 NM_001271246 NM_001271102 NM_001271101	0.0024	0.18
<i>Crem</i>	chr17:57082726:+	chr17:57088162:+	A3SS:D	NM_001271245 NM_017334 NM_001271248	0.0024	–0.18
<i>Bicd2</i>	chr17:15677426:–	chr17:15675690:–	RI:E	NM_198765	0.0048	–0.26
<i>Bicd2</i>	chr17:15677426:–	chr17:15675690:–	RI:R	NM_001033674 NM_203367	0.0048	0.26
<i>Zmynd11</i>	chr17:63831060:–	chr17:63830296:–	A5SS:P	NM_203369	0.0007	0.35
<i>Zmynd11</i>	chr17:63831060:–	chr17:63830296:–	A5SS:D	NM_203366 NM_203368	0.0007	–0.35
<i>Slc39a7</i>	chr20:3822725:–	chr20:3822427:–	RI:E	NM_001164744	0.0000	0.19
<i>Slc39a7</i>	chr20:3822725:–	chr20:3822427:–	RI:R	NM_001008885	0.0000	–0.19

For the event SE, the suffixes I and S indicate include and skip, respectively. For the event RI, the suffixes E and R indicate exclusion and retention, respectively. For the event A5SS and A3SS, the suffixes P and D indicate the use of proximal (shortened intron) and distal (extended intron) splice sites, respectively. dPSI > 0 means that the average PSI in the H120 group is larger than the average PSI in the Control group.

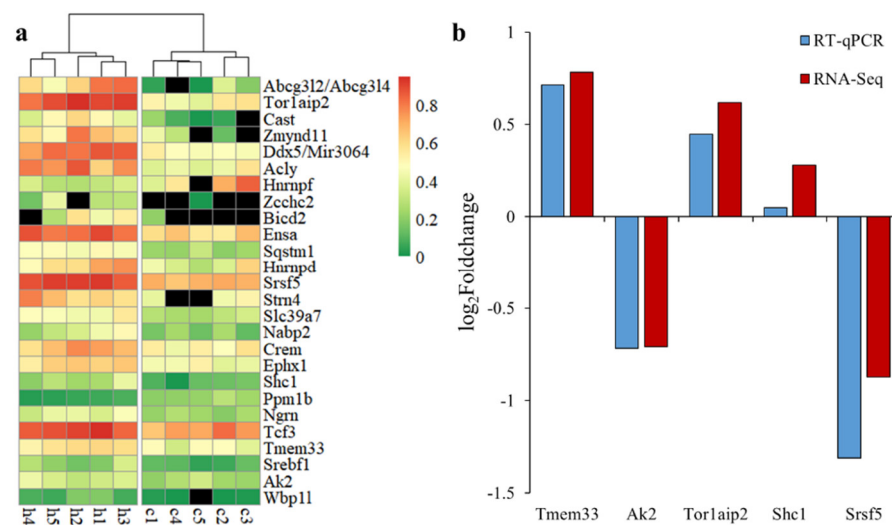


Figure 4. The expression mode of differential alternative splicing (DAS) and its expression verification. (a) heatmap of percent spliced in (PSI) values of one variant for each DAS event in the liver. The genes (top to bottom) are sorted by differences in PSI values from large to small. (b) Comparative analysis of the expression level of randomly selected DAS genes in the liver using RNA-Seq and RT-qPCR.

3.6. Functional Enrichment Analysis for Differentially Alternatively Spliced Genes

A total of 14 BPs, 6 CCs, 7 MFs and 0 pathways were annotated, of which 7 BPs, 5 CCs and 4 MFs were significantly enriched (p -value < 0.05), as shown in Table 3. Liver development (GO:0001889) containing five genes was the most significantly enriched (p -value < 0.001). Three significantly enriched BPs (GO:0032868, GO:0032869 and GO:0050796) were all related to insulin, containing four DAS genes (*Srebf1*, *Shc1*, *Srsf5* and *Ensa*). Negative regulation of transcription from the RNA polymerase II promoter (GO:0000122) was the only BP that was significantly enriched in both DEGs and DAS genes.

Table 3. Functional enrichment results of differentially alternatively spliced genes.

Group	ID	Description	p-Value	Count	Genes
BP	GO:0001889	Liver development	0.0000	5	<i>Cast, Ephx1, Ak2, Hnrnpd, Srsf5</i>
	GO:0032868	Response to insulin	0.0072	3	<i>Srebf1, Shc1, Srsf5</i>
	GO:0032869	Cellular response to insulin stimulus	0.0094	3	<i>Srebf1, Shc1, Srsf5</i>
	GO:0000122	Negative regulation of transcription from RNA polymerase II promoter	0.0109	5	<i>Srebf1, Ddx5, Tcf3, Zmynd11, Sqstm1</i>
	GO:0008610	Lipid biosynthetic process	0.0178	2	<i>Srebf1, Acly</i>
	GO:0014070	Response to organic cyclic compound	0.0415	3	<i>Srebf1, Shc1, Ephx1</i>
	GO:0050796	Regulation of insulin secretion	0.0480	2	<i>Srebf1, Ensa</i>
CC	GO:0005783	Endoplasmic reticulum	0.0051	6	<i>Cast, Srebf1, Tmem33, Tor1aip2, Slc39a7, Sqstm1</i>
	GO:0005737	Cytoplasm	0.0152	14	<i>Cast, Srebf1, Shc1, Crem, Ak2, Bcd2, Acly, Hnrnpf, Ensa, Nabp2, Srsf5, Tcf3, Sqstm1, Zcchc2</i>
	GO:0005634	Nucleus	0.0219	13	<i>Cast, Srebf1, Ddx5, Shc1, Crem, Ak2, Ngrn, Hnrnpf, Nabp2, Hnrnpd, Srsf5, Tcf3, Zmynd11</i>
	GO:0005654	Nucleoplasm	0.0307	7	<i>Acly, Ddx5, Hnrnpf, Nabp2, Hnrnpd, Slc39a7, Zmynd11</i>
	GO:0005789	Endoplasmic reticulum membrane	0.0419	4	<i>Srebf1, Tmem33, Ephx1, Tor1aip2</i>
MF	GO:0051721	Protein phosphatase 2A binding	0.0015	3	<i>Shc1, Ensa, Strn4</i>
	GO:0005515	Protein binding	0.0073	8	<i>Cast, Ddx5, Shc1, Hnrnpd, Srsf5, Tcf3, Sqstm1, Strn4</i>
	GO:0044822	Poly(A) RNA binding	0.0246	6	<i>Cast, Ngrn, Ddx5, Hnrnpf, Hnrnpd, Srsf5</i>
	GO:0003682	Chromatin binding	0.0290	4	<i>Srebf1, Hnrnpd, Tcf3, Zmynd11</i>

BP = biological process, CC = cellular component, MF = molecular function. The FDR means false discovery rate.

3.7. The Differentially Alternatively Spliced Genes with Different Expression Levels

Three DAS genes were also differentially expressed between the Control and H120 groups, accounting for 10.71% of DAS genes and 0.47% of DEGs. The hypergeometric distribution test showed that the overlap of DEGs and DAS genes was not significant ($p = 0.23$). The expression levels of *Acly* and *Hnrnpd* after heat stress (Figure 5a) were downregulated to 0.23 and 0.41 times that of the Control, respectively. The expression level of *mir3064* was upregulated to 2.35 times that of the Control. The average per-base read coverages and splice junction counts demonstrated that, after heat stress, the skipping ratio of the fourteenth exon of *Acly* and the skipping ratio of the second exon of *Hnrnpd* increased by 0.33 and 0.23 times (Figure 5b,c), respectively, and the gene expression level decreased significantly (q -value < 0.05).

Annotated alternative splice isoforms in the APPRIS Database, the two transcripts of *Acly*, including NM_016987 and NM_001111095, encode proteins with different amino acid lengths (1101 vs. 1091) and tertiary structure scores (2109.4 vs. 2067.2). The amino acid lengths of the four protein isoforms of *Hnrnpd* from long to short are 353, 334, 304 and 285, corresponding to the four transcripts NM_024404, NM_001082539, NM_001082540 and NM_001082541, respectively, and their tertiary structure scores were 413.2, 425.3, 405.08 and 417.27, respectively. The number of functional residues and domains scores of the protein isoforms of *Acly* and *Hnrnpd* have not changed, which means that alternative splicing has no effect on the function of the encoded protein.

The ATP citrate synthase encoded by *Acly* catalyzes the cleavage of citrate into oxaloacetate and acetyl-CoA, the latter serving as a common substrate for de novo cholesterol and fatty acid synthesis. *Acly* is involved in the biosynthetic processes of lipids and fatty acids and also participates in the metabolic processes of acetyl-CoA, citrate and oxaloacetate. Heterogeneous nuclear ribonucleoprotein D0 (hnRNP D0) encoded by *Hnrnpd* binds with high affinity to RNA molecules that contain AU-rich elements found within the 3'-UTR of many proto-oncogenes and cytokine mRNAs. hnRNP D0 can also bind to double- and single-stranded DNA sequences in a specific manner and functions as a transcription factor. The *Hnrnpd* can regulate gene expression at the level of transcription and translation. In addition, *Hnrnpd* plays an important role in liver development and the regulation of circadian rhythms, besides being related to cellular responses to estradiol stimuli and organonitrogen compounds.

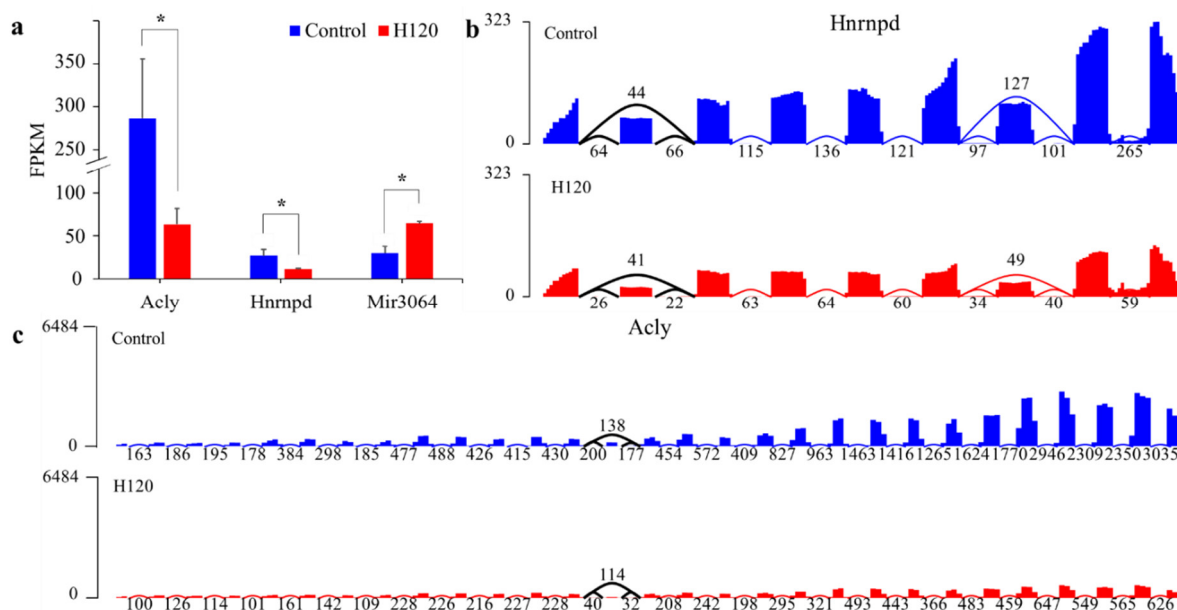


Figure 5. Expression levels of DAS genes and visualization of their splicing events. (a) The expression levels of DAS genes with different expression levels in livers in the Control and H120 groups. The asterisks (*) indicate a q -value < 0.05 and $|\log_2 \text{FoldChange}| > 1$. (b,c) The average per-base read coverages (y -axis) and splice junction counts (labels) of *Hnrnpd* and *Acly* in livers from the Control and H120 groups. The black curve indicates the location of the differential alternative splicing event.

4. Discussion

Heat-stress experiments in rats allow for easier control of experimental conditions and shorter experimental times. Based on a preliminary exploration [46], this study selected conditions of 42 °C, 50% RH (THI = 93.96) for 120 min with the strongest heat stress performance in order to simulate the physiological response state of rats under short-term, non-extreme lethal heat stress conditions [47–49]. In livestock production, the daily RH of the farm is constantly changing, and THI can more easily quantify the degree of heat stress experienced by herds. Studies have made efforts to determine the THI threshold of heat stress and the threshold has been reported variably given different physiological parameters and different production systems [50]. In the study of model animals, specific temperatures and RHs can better reflect the exact environment and contribute to the exploration of heat stress response mechanisms at the level of control variables. The flexible time setting also provides more possibilities to reveal the process of heat stress response. Studies have compared blood indicators, production performance and gene expression levels during acute and chronic heat stress [49,51,52]. Although different studies have different divisions of time, they all provide a reference for understanding the response state that changes over time during heat stress.

In this study, the liver was selected for a global transcriptome analysis to study alternative splicing induced by heat stress. The liver plays a major role in the metabolic regulation and energy balance of the stress response [53]. Therefore, studying the effects of heat stress on the liver transcriptome can help reveal the effects of heat stress on body metabolism and other aspects. To date, studies have found that heat stress has various effects on the liver. Hundreds of liver genes were differentially expressed after heat stress in different animals, including rabbits [16], fish [53,54], broilers [55] and mice [56], and the expression levels changed differently over time [57]. In addition, the alternative splicing of liver genes in fish was also affected by heat stress [32,58]. Hepatic proteins involved in the processes of heat shock response, immune defense and oxidative stress response were found to be differentially abundant when comparing heat stress with the thermal neutral zone [59]. It is reported that heat-stressed cattle have reduced albumin secretion and liver enzyme activities [60]. Previous studies have also indicated that the liver has a

higher maximum temperature than other organs during heat stress [61,62]. Liver damage caused by heatstroke is manifested as centrilobular degeneration or necrosis of hepatocytes and congestion [63]. Therefore, it is certain to have been worthwhile to select the liver for further study here.

The number of alternative splicing events and alternatively spliced genes increased after heat stress in this study, which was consistent with the research performed with fish [32]. These stress-induced increases in alternative splicing were also observed in plants [64,65] and shrimp [25]. Studies have shown that alternative splicing can improve plant tolerance to environmental stress by increasing proteome diversity [66,67]. The increase of alternative splicing may be caused by splicing errors [68,69]. Most abnormal splicing events (splicing errors) can be eliminated by mRNA monitoring mechanisms, such as nonsense mediated decay (NMD) [70,71]. Among DAS genes identified in this study, *Ngrn* produced a non-coding mRNA (NR_028055.1) whose proportion increased due to heat stress and is also a candidate for NMD [72]. *Ngrn* regulates mitochondrial 16S rRNA and intra-mitochondrial translation and is essential for oxidative phosphorylation [73]. Liver tissue may be able to increase the abundance of proteins by increasing alternative splicing to cope with heat stress, together with the mRNA monitoring mechanisms.

In this study, a total of 28 DAS genes associated with heat stress were identified and 10.71% of genes (*Acly*, *Hnrnpd* and *mir3064*) also showed significant differences in transcriptional expression (q -value < 0.05 and $|\log_2\text{FoldChange}| > 1$). This ratio was 13.4% in response to heat stress in tea leaves [24]. Therefore, for most genes, changes in alternative splicing are not the main cause of changes in gene expression and changes in alternative splicing do not necessarily lead to changes in gene expression. In *Arabidopsis thaliana*'s response to cold stress [67] and cotton's response to salt stress [64], it was also found that about two-thirds and four-fifths of differential alternative splicing did not cause differential gene expression, respectively. Zhu et al. [64] believed that the alternative splicing had an independent regulation pattern different from transcriptional regulation. These results indicate that differential expression analysis of genes and various regulatory mechanisms should be integrated to reveal the complex regulation mechanism of the heat stress response.

Among the CCs enriched by DAS genes, the endoplasmic reticulum (ER), containing six genes (*Cast*, *Srebfl1*, *Tmem33*, *Tor1aip2*, *Slc39a7* and *Sqstm1*), was most significant. ER homeostasis can be perturbed by heat stress, resulting in ER stress [74,75], and protein processing in the ER pathway is critical for the heat-stress response [54]. This study identified four DAS genes (*Srebfl1*, *Shc1*, *Srsf5* and *Ensa*) whose main functions are related to the response to insulin and regulation of insulin secretion. The increase in plasma insulin concentration after heat stress has been confirmed in cows [76], pigs [77] and rodents [78]. Heat stress-specific insulin increase appears to be adaptive and protective in nature towards stressors [2,79]. These genes may be involved in the heat stress response through alternative splicing changes.

ATP citrate lyase, encoded by *Acly*, is an important enzyme in controlling substrate supply for lipid synthesis de novo [80] and is upregulated to different degrees in many kinds of cancers [81]. The depletion of ATP citrate lyase suppressed tumor growth [82], so it has been identified as a potential molecular target for cancer therapy [83]. In this study, heat stress downregulated the expression level of DAS gene *Acly*. Similar results were found in chicken liver at the gene expression level, but heat stress increased the protein level of *Acly* [84]. However, in the heat stress of rabbits [16] and mice [56], the expression level of liver *Acly* is upregulated. Yadav et al. [85] found that the expression levels of *Acly* were regulated in different directions in different germ cells and identified *Acly* as a potential heat-sensitive target in germ cells. The *Acly* protein level in the rumen tissue of lactating dairy cows increased after chronic and mild heat stress [86]. In addition, Moon et al. [87] found that the ratios of the two mRNA isoforms of *Acly* were the same among tissues in rats and proposed that *Acly*'s alternative splicing may be related to various metabolic

diseases. This study proves that *Acly*'s alternative splicing was also significantly changed by heat stress, at the gene-expression level as well.

Hnrnpd was downregulated after heat stress in this study, as was found in limpet foot tissue [17]. The hnRNP D0 encoded by *Hnrnpd* serves as a key factor involved in mRNA decay, and there exists a significant difference among the stabilizing effects of the four isoforms [88]. hnRNP D0 may also be implicated in endothelial cell senescence [89]. Moreover, hnRNP D0 exhibits a strong response to oxidative stress; the protein decreased rapidly when cells were exposed to hydrogen peroxide [90]. As a main splicing factor involved in the formation and regulation of alternative splicing [91], *Hnrnpd* may in turn regulate the splicing of other pre-mRNAs and cause the difference of gene expression between the H120 and Control groups. *Hnrnpd* may be the predominant link between splicing regulation and heat stress response in rat livers. miRNAs play an important role in the transcriptional regulation of genes coding for proteins involved in heat-stress response-related mechanisms [92,93]. In this study, the expression of *mir3064* was significantly increased under high temperature, consistent with results for laying hens [94]. miR-3064-5p has been reported to inhibit cell proliferation and invasion in ovarian cancer [95] and to suppress angiogenesis in hepatocellular carcinoma [96]. Furthermore, a tight connection between induced oxidative stress and changed *mir3064* expression was observed in retinal pigment epithelial cells under oxidative stress conditions, suggesting that miR-3064 is a stress-responsive factor [97]. The target genes of *mir3064* regulating heat stress deserve further study.

In this study, we did not consider the unfixed duration of heat stress, the fluctuating temperature and the effect of cooling facilities, but our research results may provide a reference for research in more complex situations. Further study needs to be performed to investigate the alternative splicing events of rats exposed to different heat-stress durations and intensities. Although the liver is one of the main organs involved in the response to heat stress, it is still necessary to analyze alternative splicing event in other tissues, such as blood and adrenal glands, under heat stress to explore the mechanism of the stress response more comprehensively.

5. Conclusions

This study analyzed the changing pattern of alternative splicing in rat liver tissue under heat stress. The number of alternative splicing events under heat stress increased by 20.18%. Twenty-eight DAS genes were identified, and the molecular functions are mainly enriched in liver development and response to insulin. Three DAS genes (*Acly*, *Hnrnpd* and *mir3064*) which were differentially expressed between the Control and H120 groups can be considered as candidate markers for heat stress in rats. Taken together, these findings indicate that alternative splicing is one of the molecular mechanisms of heat stress responses in mammals.

Supplementary Materials: The following supporting information can be downloaded at: <https://www.mdpi.com/article/10.3390/genes13020358/s1>, Table S1: Primers used for real-time quantitative PCR experiment of differentially alternatively spliced genes; Table S2: Summary of RNA-Seq paired-end reads from liver tissues in Control and H120 groups; Table S3: Summary of differentially expressed genes; Table S4: Significantly enriched GO terms and pathways of differentially expressed genes.

Author Contributions: Conceptualization, Y.W. and J.D.; validation, S.H. and L.H.; formal analysis, S.H. and J.D.; investigation, J.D. and S.H.; resources, Y.Y.; data curation, J.D.; writing—original draft preparation, S.H.; writing—review and editing, J.D.; visualization, S.H.; supervision, Z.L., L.H. and Y.Y.; project administration, Y.W. and J.D.; funding acquisition, Y.W. All authors have read and agreed to the published version of the manuscript.

Funding: This research was funded by the China Agriculture Research System of MOF and MARA (no. CARS-36) and the program for the Changjiang Scholar and Innovation Research Team at the University of China (no. IRT_15R62).

Institutional Review Board Statement: All procedures and protocols for the experimental rats were approved by the Institutional Animal Care and Use Committee at the China Agricultural University, China under permission number DK996.

Informed Consent Statement: Not applicable.

Data Availability Statement: The sequence data has been submitted to the NCBI/SRA database under accession number SUB6546585.

Conflicts of Interest: The authors declare no conflict of interest.

References

- Collier, R.J.; Baumgard, L.H.; Zimbelman, R.B.; Xiao, Y. Heat stress: Physiology of acclimation and adaptation. *Anim. Front.* **2019**, *9*, 12–19. [[CrossRef](#)] [[PubMed](#)]
- Baumgard, L.H.; Rhoads, R.J. Effects of heat stress on postabsorptive metabolism and energetics. *Annu. Rev. Anim. Biosci.* **2013**, *1*, 311–337. [[CrossRef](#)] [[PubMed](#)]
- Summer, A.; Lora, I.; Formaggioni, P.; Gottardo, F. Impact of heat stress on milk and meat production. *Anim. Front.* **2019**, *9*, 39–46. [[CrossRef](#)] [[PubMed](#)]
- Sohail, M.U.; Ijaz, A.; Yousaf, M.S.; Ashraf, K.; Zaneb, H.; Aleem, M.; Rehman, H. Alleviation of cyclic heat stress in broilers by dietary supplementation of mannan-oligosaccharide and Lactobacillus-based probiotic: Dynamics of cortisol, thyroid hormones, cholesterol, C-reactive protein, and humoral immunity. *Poultry Sci.* **2010**, *89*, 1934–1938. [[CrossRef](#)]
- Mayorga, E.J.; Renaudeau, D.; Ramirez, B.C.; Ross, J.W.; Baumgard, L.H. Heat stress adaptations in pigs. *Anim. Front.* **2019**, *9*, 54–61. [[CrossRef](#)]
- Padua, J.T.; Dasilva, R.G. Effect of high environmental temperatures on weight gain and food intake of Suffolk lambs reared in a tropical environment. In Proceedings of the 5th International Symposium, Bloomington, MI, USA, 29–31 May 1997; pp. 809–815.
- Hansen, P.J. Effects of heat stress on mammalian reproduction. *Philos. Trans. R. Soc. B* **2009**, *364*, 3341–3350. [[CrossRef](#)] [[PubMed](#)]
- Lacetera, N. Impact of climate change on animal health and welfare. *Anim. Front.* **2019**, *9*, 26–31. [[CrossRef](#)]
- St-Pierre, N.R.; Cobanov, B.; Schnitkey, G. Economic Losses from Heat Stress by US Livestock Industries1. *J. Dairy Sci.* **2003**, *86*, E52–E77. [[CrossRef](#)]
- Herbut, P.; Angrecka, S. Forming of temperature-humidity index (THI) and milk production of cows in the free-stall barn during the period of summer heat. *Anim. Sci. Pap. Rep.* **2012**, *30*, 363–372.
- Lallo, C.H.O.; Cohen, J.; Rankine, D.; Taylor, M.; Cambell, J.; Stephenson, T. Characterizing heat stress on livestock using the temperature humidity index (THI)—prospects for a warmer Caribbean. *Reg. Environ. Chang.* **2018**, *18*, 2329–2340. [[CrossRef](#)]
- Dou, J.; Cánovas, A.; Brito, L.F.; Yu, Y.; Schenkel, F.S.; Wang, Y. Comprehensive RNA-Seq Profiling Reveals Temporal and Tissue-Specific Changes in Gene Expression in Sprague–Dawley Rats as Response to Heat Stress Challenges. *Front. Genet.* **2021**, *12*, 651979. [[CrossRef](#)] [[PubMed](#)]
- Liu, S.; Wang, X.; Sun, F.; Zhang, J.; Feng, J.; Liu, H.; Rajendran, K.V.; Sun, L.; Zhang, Y.; Jiang, Y.; et al. RNA-Seq reveals expression signatures of genes involved in oxygen transport, protein synthesis, folding, and degradation in response to heat stress in catfish. *Physiol. Genom.* **2013**, *45*, 462–476. [[CrossRef](#)] [[PubMed](#)]
- Dou, J.; Khan, A.; Khan, M.Z.; Mi, S.; Wang, Y.; Yu, Y.; Wang, Y. Heat Stress Impairs the Physiological Responses and Regulates Genes Coding for Extracellular Exosomal Proteins in Rat. *Genes* **2020**, *11*, 306. [[CrossRef](#)] [[PubMed](#)]
- Dado-Senn, B.; Skibieli, A.L.; Fabris, T.F.; Zhang, Y.; Dahl, G.E.; Penagaricano, F.; Laporta, J. RNA-Seq reveals novel genes and pathways involved in bovine mammary involution during the dry period and under environmental heat stress. *Sci. Rep.* **2018**, *8*, 11096. [[CrossRef](#)]
- Wu, Z.L.; Yang, X.; Chen, S.Y.; Deng, F.L.; Jia, X.B.; Hu, S.Q.; Wang, J.; Lai, S.J. Liver Transcriptome Changes of Hyla Rabbit in Response to Chronic Heat Stress. *Animals* **2019**, *9*, 1141. [[CrossRef](#)]
- Moreira, C.; Stillman, J.H.; Lima, F.P.; Xavier, R.; Seabra, R.; Gomes, F.; Verissimo, A.; Silva, S.M. Transcriptomic response of the intertidal limpet *Patella vulgata* to temperature extremes. *J. Therm. Biol.* **2021**, *101*, 103096. [[CrossRef](#)]
- Gilbert, W. Why Genes in Pieces? *Nature* **1978**, *271*, 501. [[CrossRef](#)]
- Chen, M.; Manley, J.L. Mechanisms of alternative splicing regulation: Insights from molecular and genomics approaches. *Nat. Rev. Mol. Cell Biol.* **2009**, *10*, 741–754. [[CrossRef](#)]
- Black, D.L. Mechanisms of alternative pre-messenger RNA splicing. *Annu. Rev. Biochem.* **2003**, *72*, 291–336. [[CrossRef](#)]
- Laloum, T.; Martin, G.; Duque, P. Alternative Splicing Control of Abiotic Stress Responses. *Trends Plant Sci.* **2018**, *23*, 140–150. [[CrossRef](#)]
- Staiger, D.; Brown, J.W. Alternative splicing at the intersection of biological timing, development, and stress responses. *Plant Cell* **2013**, *25*, 3640–3656. [[CrossRef](#)] [[PubMed](#)]
- Mastrangelo, A.M.; Marone, D.; Laido, G.; De Leonardis, A.M.; De Vita, P. Alternative splicing: Enhancing ability to cope with stress via transcriptome plasticity. *Plant Sci.* **2012**, *185–186*, 40–49. [[CrossRef](#)] [[PubMed](#)]
- Ding, Y.; Wang, Y.; Qiu, C.; Qian, W.; Xie, H.; Ding, Z. Alternative splicing in tea plants was extensively triggered by drought, heat and their combined stresses. *PeerJ* **2020**, *8*, e8258. [[CrossRef](#)]

25. Zhang, X.; Yuan, J.; Zhang, X.; Liu, C.; Xiang, J.; Li, F. Genome-Wide Analysis of Alternative Splicing Provides Insights Into Stress Response of the Pacific White Shrimp *Litopenaeus vannamei*. *Front. Genet.* **2019**, *10*, 845. [[CrossRef](#)] [[PubMed](#)]
26. Takechi, H.; Hosokawa, N.; Hirayoshi, K.; Nagata, K. Alternative 5' splice site selection induced by heat shock. *Mol. Cell Biol.* **1994**, *14*, 567–575. [[CrossRef](#)]
27. Nevo, Y.; Kamhi, E.; Jacob-Hirsch, J.; Amariglio, N.; Rechavi, G.; Sperling, J.; Sperling, R. Genome-wide activation of latent donor splice sites in stress and disease. *Nucleic Acids Res.* **2012**, *40*, 10980–10994. [[CrossRef](#)] [[PubMed](#)]
28. Nevo, Y.; Sperling, J.; Sperling, R. Heat shock activates splicing at latent alternative 5' splice sites in nematodes. *Nucleus* **2015**, *6*, 225–235. [[CrossRef](#)]
29. Ju, X.; Xu, H.; Yong, Y.; An, L.; Xu, Y.; Jiao, P.; Liao, M. Heat Stress Upregulates the Expression of TLR4 and Its Alternative Splicing Variant in Bama Miniature Pigs. *J. Integr. Agr.* **2014**, *13*, 2479–2487. [[CrossRef](#)]
30. Fujikake, N.; Nagai, Y.; Popiel, H.A.; Kano, H.; Yamaguchi, M.; Toda, T. Alternative splicing regulates the transcriptional activity of Drosophila heat shock transcription factor in response to heat/cold stress. *FEBS Lett.* **2005**, *579*, 3842–3848. [[CrossRef](#)]
31. Kaitsuka, T.; Tomizawa, K.; Matsushita, M. Transformation of eEF1Bdelta into heat-shock response transcription factor by alternative splicing. *EMBO Rep.* **2011**, *12*, 673–681. [[CrossRef](#)]
32. Tan, S.; Wang, W.; Tian, C.; Niu, D.; Zhou, T.; Jin, Y.; Yang, Y.; Gao, D.; Dunham, R.; Liu, Z. Heat stress induced alternative splicing in catfish as determined by transcriptome analysis. *Comp. Biochem. Physiol. Part D Genom. Proteom.* **2019**, *29*, 166–172. [[CrossRef](#)] [[PubMed](#)]
33. Kang, S.W.; Madkour, M.; Kuenzel, W.J. Tissue-Specific Expression of DNA Methyltransferases Involved in Early-Life Nutritional Stress of Chicken, *Gallus gallus*. *Front. Genet.* **2017**, *8*, 204. [[CrossRef](#)] [[PubMed](#)]
34. Madkour, M.; Aboelenin, M.M.; Aboelazab, O.; Elolimy, A.A.; El-Azeem, N.A.; El-Kholy, M.S.; Alagawany, M.; Shourrap, M. Hepatic expression responses of DNA methyltransferases, heat shock proteins, antioxidant enzymes, and NADPH 4 to early life thermal conditioning in broiler chickens. *Ital. J. Anim. Sci.* **2021**, *20*, 433–446. [[CrossRef](#)]
35. Hadfield, J.; Eldridge, M.D. Multi-genome alignment for quality control and contamination screening of next-generation sequencing data. *Front. Genet.* **2014**, *5*, 31. [[CrossRef](#)]
36. Dobin, A.; Davis, C.A.; Schlesinger, F.; Drenkow, J.; Zaleski, C.; Jha, S.; Batut, P.; Chaisson, M.; Gingeras, T.R. STAR: Ultrafast universal RNA-seq aligner. *Bioinformatics* **2013**, *29*, 15–21. [[CrossRef](#)]
37. Pertea, M.; Pertea, G.M.; Antonescu, C.M.; Chang, T.C.; Mendell, J.T.; Salzberg, S.L. StringTie enables improved reconstruction of a transcriptome from RNA-seq reads. *Nat. Biotechnol.* **2015**, *33*, 290–295. [[CrossRef](#)]
38. Pertea, M.; Kim, D.; Pertea, G.M.; Leek, J.T.; Salzberg, S.L. Transcript-level expression analysis of RNA-seq experiments with HISAT, StringTie and Ballgown. *Nat. Protoc.* **2016**, *11*, 1650–1667. [[CrossRef](#)]
39. Goldstein, L.D.; Cao, Y.; Pau, G.; Lawrence, M.; Wu, T.D.; Seshagiri, S.; Gentleman, R. Prediction and Quantification of Splice Events from RNA-Seq Data. *PLoS ONE* **2016**, *11*, e156132. [[CrossRef](#)]
40. Anders, S.; Reyes, A.; Huber, W. Detecting differential usage of exons from RNA-seq data. *Genome Res.* **2012**, *22*, 2008–2017. [[CrossRef](#)]
41. Rodriguez, J.M.; Maietta, P.; Ezkurdia, I.; Pietrelli, A.; Wesselink, J.J.; Lopez, G.; Valencia, A.; Tress, M.L. APPRIS: Annotation of principal and alternative splice isoforms. *Nucleic Acids Res.* **2013**, *41*, D110–D117. [[CrossRef](#)]
42. Huang, D.W.; Sherman, B.T.; Lempicki, R.A. Bioinformatics enrichment tools: Paths toward the comprehensive functional analysis of large gene lists. *Nucleic Acids Res.* **2009**, *37*, 1–13. [[CrossRef](#)] [[PubMed](#)]
43. UP Consortium. UniProt: The universal protein knowledgebase in 2021. *Nucleic Acids Res.* **2021**, *49*, D480–D489. [[CrossRef](#)] [[PubMed](#)]
44. Smith, J.R.; Hayman, G.T.; Wang, S.J.; Laulederkind, S.; Hoffman, M.J.; Kaldunski, M.L.; Tutaj, M.; Thota, J.; Nalabolu, H.S.; Ellanki, S.; et al. The Year of the Rat: The Rat Genome Database at 20: A multi-species knowledgebase and analysis platform. *Nucleic Acids Res.* **2020**, *48*, D731–D742. [[CrossRef](#)]
45. Ye, J.; Coulouris, G.; Zaretskaya, I.; Cutcutache, I.; Rozen, S.; Madden, T.L. Primer-BLAST: A tool to design target-specific primers for polymerase chain reaction. *BMC Bioinform.* **2012**, *13*, 134. [[CrossRef](#)] [[PubMed](#)]
46. Dou, J.; Montanholi, Y.R.; Wang, Z.; Li, Z.; Yu, Y.; Martell, J.E.; Wang, Y.J.; Wang, Y. Corticosterone tissue-specific response in Sprague Dawley rats under acute heat stress. *J. Therm. Biol.* **2019**, *81*, 12–19. [[CrossRef](#)] [[PubMed](#)]
47. Qu, Q.; Li, H.; Bai, L.; Zhang, S.; Sun, J.; Lv, W.; Ye, C.; Liu, C.; Shi, D. Effects of Heat Stress on Gut Microbiome in Rats. *Indian J. Microbiol.* **2021**, *61*, 338–347. [[CrossRef](#)]
48. Yu, J.; Liu, F.; Yin, P.; Zhu, X.; Cheng, G.; Wang, N.; Lu, A.; Luan, W.; Zhang, N.; Li, J.; et al. Integrating miRNA and mRNA expression profiles in response to heat stress-induced injury in rat small intestine. *Funct. Integr. Genom.* **2011**, *11*, 203–213. [[CrossRef](#)]
49. Sinha, R.K. Study of changes in some pathophysiological stress markers in different age groups of an animal model of acute and chronic heat stress. *Iran. Biomed. J.* **2007**, *11*, 101–111.
50. Sammad, A.; Wang, Y.J.; Umer, S.; Lirong, H.; Khan, I.; Khan, A.; Ahmad, B.; Wang, Y. Nutritional Physiology and Biochemistry of Dairy Cattle under the Influence of Heat Stress: Consequences and Opportunities. *Animals* **2020**, *10*, 793. [[CrossRef](#)]
51. Barrett, N.W.; Rowland, K.; Schmidt, C.J.; Lamont, S.J.; Rothschild, M.F.; Ashwell, C.M.; Persia, M.E. Effects of acute and chronic heat stress on the performance, egg quality, body temperature, and blood gas parameters of laying hens. *Poult. Sci.* **2019**, *98*, 6684–6692. [[CrossRef](#)]

52. Xie, J.; Tang, L.; Lu, L.; Zhang, L.; Xi, L.; Liu, H.C.; Odle, J.; Luo, X. Differential expression of heat shock transcription factors and heat shock proteins after acute and chronic heat stress in laying chickens (*Gallus gallus*). *PLoS ONE* **2014**, *9*, e102204. [[CrossRef](#)]
53. Vijayan, M.M. Gene expression pattern in the liver during recovery from an acute stressor in rainbow trout. *Comp. Biochem. Physiol. Part D Genom. Proteom.* **2007**, *2*, 244.
54. Wang, Y.; Li, C.; Pan, C.; Liu, E.; Zhao, X.; Ling, Q. Alterations to transcriptomic profile, histopathology, and oxidative stress in liver of pikeperch (*Sander luciopeca*) under heat stress. *Fish Shellfish. Immunol.* **2019**, *95*, 659–669. [[CrossRef](#)] [[PubMed](#)]
55. Yu, J.; Bao, E. Effect of acute heat stress on heat shock protein 70 and its corresponding mRNA expression in the heart, liver, and kidney of broilers. *Asian Austral. J. Anim.* **2008**, *21*, 1116–1126. [[CrossRef](#)]
56. Bhusari, S.; Liu, Z.; Hearne, L.B.; Spiers, D.E.; Lamberson, W.R.; Antoniou, E. Expression profiling of heat stress effects on mice fed ergot alkaloids. *Toxicol. Sci.* **2007**, *95*, 89–97. [[CrossRef](#)] [[PubMed](#)]
57. Purohit, G.K.; Mahanty, A.; Suar, M.; Sharma, A.P.; Mohanty, B.P.; Mohanty, S. Investigating hsp gene expression in liver of *Channa striatus* under heat stress for understanding the upper thermal acclimation. *Biomed Res. Int.* **2014**, *2014*, 381719. [[CrossRef](#)] [[PubMed](#)]
58. Rabergh, C.M.; Airaksinen, S.; Soitamo, A.; Bjorklund, H.V.; Johansson, T.; Nikinmaa, M.; Sistonen, L. Tissue-specific expression of zebrafish (*Danio rerio*) heat shock factor 1 mRNAs in response to heat stress. *J. Exp. Biol.* **2000**, *203*, 1817–1824. [[CrossRef](#)]
59. Cui, Y.; Hao, Y.; Li, J.; Bao, W.; Li, G.; Gao, Y.; Gu, X. Chronic Heat Stress Induces Immune Response, Oxidative Stress Response, and Apoptosis of Finishing Pig Liver: A Proteomic Approach. *Int. J. Mol. Sci.* **2016**, *17*, 393. [[CrossRef](#)]
60. Ronchi, B.; Bernabucci, U.; Lacetera, N.; Verini Supplizi, A.; Nardone, A. Distinct and common effects of heat stress and restricted feeding on metabolic status of Holstein heifers. *Zootec. E Nutr. Anim.* **1999**, *25*, 11–20.
61. Rakesh, V.; Stallings, J.D.; Helwig, B.G.; Leon, L.R.; Jackson, D.A.; Reifman, J. A 3-D mathematical model to identify organ-specific risks in rats during thermal stress. *J Appl. Physiol.* **2013**, *115*, 1822–1837. [[CrossRef](#)]
62. Lin, H.; Decuyper, E.; Buyse, J. Acute heat stress induces oxidative stress in broiler chickens. *Comp. Biochem. Physiol. A Mol. Integr. Physiol.* **2006**, *144*, 11–17. [[CrossRef](#)] [[PubMed](#)]
63. Kew, M.; Bersohn, I.; Seftel, H.; Kent, G. Liver damage in heatstroke. *Am. J. Med.* **1970**, *49*, 192–202. [[CrossRef](#)]
64. Zhu, G.; Li, W.; Zhang, F.; Guo, W. RNA-seq analysis reveals alternative splicing under salt stress in cotton, *Gossypium davidsonii*. *BMC Genom.* **2018**, *19*, 73. [[CrossRef](#)] [[PubMed](#)]
65. Feng, J.; Li, J.; Gao, Z.; Lu, Y.; Yu, J.; Zheng, Q.; Yan, S.; Zhang, W.; He, H.; Ma, L.; et al. SKIP Confers Osmotic Tolerance during Salt Stress by Controlling Alternative Gene Splicing in Arabidopsis. *Mol. Plant* **2015**, *8*, 1038–1052. [[CrossRef](#)] [[PubMed](#)]
66. Syed, N.H.; Kalyna, M.; Marquez, Y.; Barta, A.; Brown, J.W. Alternative splicing in plants—coming of age. *Trends Plant Sci.* **2012**, *17*, 616–623. [[CrossRef](#)] [[PubMed](#)]
67. Calixto, C.P.G.; Guo, W.; James, A.B.; Tzioutziou, N.A.; Entizne, J.C.; Panter, P.E.; Knight, H.; Nimmo, H.G.; Zhang, R.; Brown, J.W.S. Rapid and Dynamic Alternative Splicing Impacts the Arabidopsis Cold Response Transcriptome. *Plant Cell* **2018**, *30*, 1424–1444. [[CrossRef](#)] [[PubMed](#)]
68. Ding, F.; Cui, P.; Wang, Z.; Zhang, S.; Ali, S.; Xiong, L. Genome-wide analysis of alternative splicing of pre-mRNA under salt stress in Arabidopsis. *BMC Genom.* **2014**, *15*, 431. [[CrossRef](#)]
69. Cui, P.; Zhang, S.; Ding, F.; Ali, S.; Xiong, L. Dynamic regulation of genome-wide pre-mRNA splicing and stress tolerance by the Sm-like protein Lsm5 in Arabidopsis. *Genome Biol.* **2014**, *15*, R1. [[CrossRef](#)]
70. Chang, Y.F.; Imam, J.S.; Wilkinson, M.F. The nonsense-mediated decay RNA surveillance pathway. *Annu. Rev. Biochem.* **2007**, *76*, 51–74. [[CrossRef](#)]
71. Cartegni, L.; Chew, S.L.; Krainer, A.R. Listening to silence and understanding nonsense: Exonic mutations that affect splicing. *Nat. Rev. Genet.* **2002**, *3*, 285–298. [[CrossRef](#)]
72. Benson, D.A.; Cavanaugh, M.; Clark, K.; Karsch-Mizrachi, I.; Lipman, D.J.; Ostell, J.; Sayers, E.W. GenBank. *Nucleic Acids Res.* **2013**, *41*, D36–D42. [[CrossRef](#)] [[PubMed](#)]
73. Arroyo, J.D.; Jourdain, A.A.; Calvo, S.E.; Ballarano, C.A.; Doench, J.G.; Root, D.E.; Mootha, V.K. A Genome-wide CRISPR Death Screen Identifies Genes Essential for Oxidative Phosphorylation. *Cell Metab.* **2016**, *24*, 875–885. [[CrossRef](#)] [[PubMed](#)]
74. Osowski, C.M.; Urano, F. Measuring ER stress and the unfolded protein response using mammalian tissue culture system. *Methods Enzym.* **2011**, *490*, 71–92. [[CrossRef](#)]
75. Alemu, T.W.; Pandey, H.O.; Salilew, W.D.; Gebremedhn, S.; Neuhof, C.; Tholen, E.; Holker, M.; Schellander, K.; Tesfaye, D. Oxidative and endoplasmic reticulum stress defense mechanisms of bovine granulosa cells exposed to heat stress. *Theriogenology* **2018**, *110*, 130–141. [[CrossRef](#)] [[PubMed](#)]
76. Wheelock, J.B.; Rhoads, R.P.; Vanbaale, M.J.; Sanders, S.R.; Baumgard, L.H. Effects of heat stress on energetic metabolism in lactating Holstein cows. *J. Dairy Sci.* **2010**, *93*, 644–655. [[CrossRef](#)]
77. Pearce, S.C.; Gabler, N.K.; Ross, J.W.; Escobar, J.; Patience, J.F.; Rhoads, R.P.; Baumgard, L.H. The effects of heat stress and plane of nutrition on metabolism in growing pigs. *J. Anim. Sci.* **2013**, *91*, 2108–2118. [[CrossRef](#)]
78. Torlinska, T.; Banach, R.; Paluszak, J.; Gryczka-Dziadecka, A. Hyperthermia effect on lipolytic processes in rat blood and adipose tissue. *Acta Physiol. Pol.* **1987**, *38*, 361–366.
79. Geiger, P.C.; Gupte, A.A. Heat shock proteins are important mediators of skeletal muscle insulin sensitivity. *Exerc. Sport Sci. Rev.* **2011**, *39*, 34–42. [[CrossRef](#)]

80. Pearce, N.J.; Yates, J.W.; Berkhout, T.A.; Jackson, B.; Tew, D.; Boyd, H.; Camilleri, P.; Sweeney, P.; Gribble, A.D.; Shaw, A.; et al. The role of ATP citrate-lyase in the metabolic regulation of plasma lipids. Hypolipidaemic effects of SB-204990, a lactone prodrug of the potent ATP citrate-lyase inhibitor SB-201076. *Biochem. J.* **1998**, *334 Pt 1*, 113–119. [[CrossRef](#)]
81. Xin, M.; Qiao, Z.; Li, J.; Liu, J.; Song, S.; Zhao, X.; Miao, P.; Tang, T.; Wang, L.; Liu, W.; et al. miR-22 inhibits tumor growth and metastasis by targeting ATP citrate lyase: Evidence in osteosarcoma, prostate cancer, cervical cancer and lung cancer. *Oncotarget* **2016**, *7*, 44252–44265. [[CrossRef](#)]
82. Wang, D.; Yin, L.; Wei, J.; Yang, Z.; Jiang, G. ATP citrate lyase is increased in human breast cancer, depletion of which promotes apoptosis. *Tumour. Biol.* **2017**, *39*, 1393391326. [[CrossRef](#)] [[PubMed](#)]
83. Hatzivassiliou, G.; Zhao, F.; Bauer, D.E.; Andreadis, C.; Shaw, A.N.; Dhanak, D.; Hingorani, S.R.; Tuveson, D.A.; Thompson, C.B. ATP citrate lyase inhibition can suppress tumor cell growth. *Cancer Cell* **2005**, *8*, 311–321. [[CrossRef](#)] [[PubMed](#)]
84. Flees, J.; Rajaei-Sharifabadi, H.; Greene, E.; Beer, L.; Hargis, B.M.; Ellestad, L.; Porter, T.; Donoghue, A.; Bottje, W.G.; Dridi, S. Effect of *Morinda citrifolia* (Noni)-Enriched Diet on Hepatic Heat Shock Protein and Lipid Metabolism-Related Genes in Heat Stressed Broiler Chickens. *Front. Physiol.* **2017**, *8*, 919. [[CrossRef](#)]
85. Yadav, S.K.; Pandey, A.; Kumar, L.; Devi, A.; Kushwaha, B.; Vishvkarma, R.; Maikhuri, J.P.; Rajender, S.; Gupta, G. The thermo-sensitive gene expression signatures of spermatogenesis. *Reprod. Biol. Endocrinol.* **2018**, *16*, 56. [[CrossRef](#)] [[PubMed](#)]
86. Eslamizad, M.; Albrecht, D.; Kuhla, B. The effect of chronic, mild heat stress on metabolic changes of nutrition and adaptations in rumen papillae of lactating dairy cows. *J. Dairy Sci.* **2020**, *103*, 8601–8614. [[CrossRef](#)]
87. Moon, Y.A.; Kim, K.S.; Park, S.W.; Kim, Y.S. Cloning and identification of exon-intron organization of the rat ATP-citrate lyase gene. *Biochim. Biophys. Acta* **1996**, *1307*, 280–284. [[CrossRef](#)]
88. Xu, N.; Chen, C.Y.; Shyu, A.B. Versatile role for hnRNP D isoforms in the differential regulation of cytoplasmic mRNA turnover. *Mol. Cell. Biol.* **2001**, *21*, 6960–6971. [[CrossRef](#)]
89. Latorre, E.; Torregrossa, R.; Wood, M.E.; Whiteman, M.; Harries, L.W. Mitochondria-targeted hydrogen sulfide attenuates endothelial senescence by selective induction of splicing factors HNRNP D and SRSF2. *Aging* **2018**, *10*, 1666–1681. [[CrossRef](#)]
90. Hayakawa, H.; Fujikane, A.; Ito, R.; Matsumoto, M.; Nakayama, K.I.; Sekiguchi, M. Human proteins that specifically bind to 8-oxoguanine-containing RNA and their responses to oxidative stress. *Biochem. Biophys. Res. Commun.* **2010**, *403*, 220–224. [[CrossRef](#)]
91. Lee, Y.; Rio, D.C. Mechanisms and Regulation of Alternative Pre-mRNA Splicing. *Annu. Rev. Biochem.* **2015**, *84*, 291–323. [[CrossRef](#)]
92. Zheng, Y.; Chen, K.L.; Zheng, X.M.; Li, H.X.; Wang, G.L. Identification and bioinformatics analysis of microRNAs associated with stress and immune response in serum of heat-stressed and normal Holstein cows. *Cell Stress Chaperones* **2014**, *19*, 973–981. [[CrossRef](#)] [[PubMed](#)]
93. Li, Q.; Yang, C.; Du, J.; Zhang, B.; He, Y.; Hu, Q.; Li, M.; Zhang, Y.; Wang, C.; Zhong, J. Characterization of miRNA profiles in the mammary tissue of dairy cattle in response to heat stress. *BMC Genom.* **2018**, *19*, 975. [[CrossRef](#)] [[PubMed](#)]
94. Zhu, L.; Liao, R.; Wu, N.; Zhu, G.; Tu, Y.; Yang, C. Integrating miRNA and mRNA expression profiles in plasma of laying hens associated with heat stress. *Mol. Biol. Rep.* **2019**, *46*, 2779–2789. [[CrossRef](#)] [[PubMed](#)]
95. Bai, L.; Wang, H.; Wang, A.H.; Zhang, L.Y.; Bai, J. MicroRNA-532 and microRNA-3064 inhibit cell proliferation and invasion by acting as direct regulators of human telomerase reverse transcriptase in ovarian cancer. *PLoS ONE* **2017**, *12*, e173912. [[CrossRef](#)]
96. Zhang, P.; Ha, M.; Li, L.; Huang, X.; Liu, C. MicroRNA-3064-5p sponged by MALAT1 suppresses angiogenesis in human hepatocellular carcinoma by targeting the FOXA1/CD24/Src pathway. *FASEB J.* **2020**, *34*, 66–81. [[CrossRef](#)]
97. Donato, L.; Bramanti, P.; Scimone, C.; Rinaldi, C.; Giorgianni, F.; Beranova-Giorgianni, S.; Koirala, D.; D’Angelo, R.; Sidoti, A. miRNA expression profile of retinal pigment epithelial cells under oxidative stress conditions. *FEBS Open Bio* **2018**, *8*, 219–233. [[CrossRef](#)]